Characterisation of Free Volume in Amorphous Materials by PALS in Relation to Relaxation Phenomena

G. Dlubek[1*], D. Kilburn[2], V. Bondarenko[3], J. Pionteck[4], R. Krause-Rehberg[3], M. A. Alam[2]

[1]ITA Institut für Innovative Technologien, Köthen/Halle, Wiesenring 4, D-06120 Lieskau (bei Halle/S.), Germany (gdlubek@aol.com, Tel.: +49-345-5512902)
[2]H.H.Wills Physics Lab., University of Bristol, Tyndall Avenue, Bristol, BS8 1TL, UK
[3]Martin-Luther-Universität Halle-Wittenberg, Fachbereich Physik, D-06099 Halle/S,
[4]Institut für Polymerforschung Dresden e.V., Hohe Strasse 6, D-01069 Dresden, Germany

1. Introduction

The volume of solids and liquids can not be filled to 100 % by atoms owing to their spherical shape. A unoccupied free volume appears, its specific value V_f and fraction f can be calculated from

$$V_f = V - V_{occ}, \qquad f = 1 - V_{occ}/V \tag{1}$$

where V and V_{occ} are the specific total and occupied volumes. Identifying V_{occ} with the van der Waals volume of atoms or molecules, V_W, the total free volume can be calculated from eq. (1), $V_{fW} = V - V_W$, $f_W = 1 - V_W/V$. This empty space appears in crystals and is denoted here as interstitial free volume, V_{fi}, with its fraction f_i [1]. In the following we will focus our discussion on polymers. For polymer crystals f_i has typical values somewhat larger than in the most dense packing (hdp or fcc) of hard spheres, $f_i > 0.26$. In amorphous polymers an additional or excess free volume appears due to the (static or dynamic) structural disorder [2-4]. This excess free volume appears as many small holes (h) and can be calculated from eq. (1) assuming $V_{occ} = V_c$, $V_{fh} = V - V_c$, where V_c (= $V_W + V_{fi}$) is specific volume of the corresponding crystal. The excess free volume fraction is $f_h = 1 - V_c/V$. Following the traditional terminology we will use the symbols V_f (≡ V_{fh}) and f (≡ f_h ≡ h) to describe the excess free volume and its volume fraction in the following paragraphs.

Computer simulation of the amorphous polymer structure shows that the unoccupied, empty volume is a single space which is constituted by a large number of multi-interconnected subnanometer size free volumes [5,6]. These local free volumes are of irregular shape and different size. If a probe molecule is inserted, the empty space decays into isolated small local free volumes (holes). The integral volume fraction of these "probed" holes decreases in an exponential-like way with the size of the probe molecule. The holes of the excess free volume play an important role in the polymer dynamics observed via dielectrical or mechanical relaxation experiments and in the diffusion of small molecules.

Most of the traditional free-volume concepts of diffusion of small molecules in liquids start with the theory of Cohen and Turnbull [4], or modified versions of this. This theory, which is also successfully applied to polymers assumes that molecular transport occurs in a liquid of hard spheres by the movement of a molecule into a hole within a cage delineated by the immediate neighbours of the moving particle when the hole has a greater size than some critical value v^*. The holes are formed by a redistribution of the free volume arising from the co-operative thermal motion of neighbour atoms. No energy in the sense of an activation energy is required for free volume redistribution. Applying statistical mechanics the distribution function of local free volumes is found to be [4]

$$p(v) = (\gamma/v_f)\exp(-\gamma v/v_f) \quad (2)$$

where v is the volume of an individual hole and v_f denotes the mean free volume per molecule. γ is a numerical factor between 0.5 and unity, and is used to correct for the overlapping of holes. The probability of finding a hole of volume v^* or larger is given by $\exp(-\gamma v^*/v_f)$ which is obtained from the integration of eq. (2) from v^* to ∞.

Using this probability the average diffusion coefficient may be written as $D \sim u \exp(-\gamma v^*/v_f)$. The diffusing molecule is assumed to move across the hole within its cage with a velocity $u \propto T^{1/2}$. Looking, for example, to the mobility of ions in a polymer and applying the Nernst-Einstein equation, the ionic conductivity σ is then given by

$$\sigma = C\, T^{-1/2} \exp(-\gamma v^*/v_f) \quad . \quad (3)$$

Here C and γv^* are fitting parameters and are assumed to be constant. It may be assumed that the free volume v_f increases linearly with the temperature for $T > T_g$,

$$v_f = (dv_f/dT)(T-T_0') = \alpha_f^* v_m (T-T_0') \quad (4)$$

where T_0' is the temperature at which the extrapolated (hypothetical equilibrium) free volume disappears. $\alpha_f^* = (1/v_m)dv_f/dT$ is the fractional coefficient of the thermal expansion of the free volume and v_m is the molecular volume. By substituting eq. (4) into (3), one obtains the well known Vogel-Tammann-Fulcher (VTF) equation, here for ionic conductivity,

$$\sigma(T) = A\, T^{-1/2} \exp\{-B/R(T - T_0)\} \; . \quad (5)$$

R is the gas constant and A, B, and T_0 are fitting constants. B may be considered as a pseudo activation energy. T_0 (Vogel temperature) is the temperature where the (extrapolated) mobility of ions will disappear. The eqs. (3-5) link the mobility properties with free volume properties, $B/R = [\gamma v^*/(dv_f/dT)] = (\gamma v^*/v_m \alpha_f^*)$ and $T_0 = T_0'$. An equation like eq. (5) is also used to describe the α- (segmental) and other relaxation processes in polymers [10]. Eqs. (3-5) tell us that only a fraction, $\exp(-\gamma v^*/v_f)$, of the total free volume is associated with a movement and that this fraction depends on the type and size of the moving species (small molecules or polymer chain segments, for example). This point is sometimes ignored when linking mobility and free volume properties. We remark moreover, that the excess free volume, V_f, and the occupied volume that contains the interstitial free volume, $V_{occ} = V_W + V_{fi}$, show different behaviour with respect to thermal expansion and isothermal compression. Thus, the frequently made observation of different relaxation properties for the same total volume or density does not necessarily contradict free volume theory. The total volume is not the controlling parameter of the mobility, but the correct $V_f = V_f(v^*, v_f)$ is. V_f depends on the route in the T-P plane on which the constant V is reached.

While the relaxation properties of amorphous polymers are usually well known [10], only limited information are available about the microstructure of the free volume: the hole dimensions, number densities and the size and shape distribution. This is mainly due to a lack of suitable probes for open volumes of molecular dimensions. A unique tool to probe such holes is the positron (positronium) annihilation spectroscopy (PALS) [7-9].

In molecular materials a significant fraction of the injected positrons annihilates from the positronium (Ps) bound state. The Ps forms either in the so called para (anti-parallel

electron and positron spins: p-Ps) or ortho (parallel electron and positron spins: o-Ps) states with a relative abundance of 1:3. In vacuum, p-Ps has a lifetime of 125 ps and annihilates via 2 γ-photons while o-Ps lives 142 ns and annihilates via 3 γ-photons [7,8].

When within the free volume in polymers, the o-Ps has a finite probability of annihilating with an electron other than its bound partner (and of opposite spin) during the numerous collisions that it undergoes with the molecules of the surrounding material, a process generally known as the 'pick-off'. The result is a sharply reduced o-Ps lifetime depending on the frequency of collisions. The collision frequency of the Ps with the surrounding molecules will depend on the dimensions of the confining volume. This results in a highly sensitive correspondence of the o-Ps pick-off rate, and therefore the lifetime, to the free volume hole size [5-8]. In this paper we present a short introduction in the positron annihilation techniques and give an overview of applications for studying free-volume properties of amorphous polymers in close relation to relaxation properties.

2. The Positron Annihilation Techniques

Positrons are supplied by radioactive sources such as ^{22}Na with high kinetic energies (Fig. 1). If implanted into a solid the fast positrons slow down within a few ps due to ionisation and excitation of molecules. The implantation profile of positrons is an exponentially decreasing function $\exp(-\alpha x)$ where α = 42 cm^{-1} is the positron absorption coefficient (in materials of density 1 g/cm^3) and x is the depth where the positron is stopped. 50, 90 and 99 % of implanted positrons are stopped at depths of 0.17, 0.55 and 1.1 mm. Thin polymer foils may be stacked to obtain the required thickness of sample. The free (not Ps) positrons annihilate via emission of two (almost co-linear) γ-photons of 0.51 MeV energy. Simultaneously with the emission of the positron the ^{22}Na nucleus emits a 1.3 MeV photon. The time delay between the 1.3 MeV (start γ , positron birth) and the 0. 51 MeV photons (stop γ, positron annihilation), i. e. the lifetime of a positron, can be measured with a positron annihilation lifetime spectrometer (PALS) using two fast scintillation detectors. The momentum distribution of e^+-e^- pairs can be determined either by measuring the Doppler-broadening of the 0.51 MeV annihilation radiation (DBAR) using a Ge detector, or the 2γ angular correlation of annihilation radiation (ACAR, Fig. 1) [7-9].

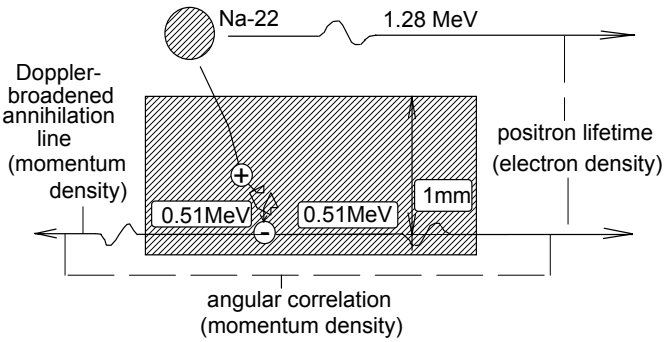

Figure 1. The positron experiments.

While the lifetime of an individual positron may vary between 0 and ∞, the lifetime spectrum of an ensemble of positrons annihilating from a solitary state is a single exponential $\exp(-t/\tau)$ where τ denotes the characteristic (mean) lifetime of positrons. As shown in Fig. 2, typically three lifetime components appear in amorphous polymers:

$$s(t) = \sum(I_i/\tau_i)\exp(-t/\tau_i), \qquad \sum I_i = 1, \qquad (i = 1...3). \tag{6}$$

These lifetimes arise from annihilation of p-Ps (τ_1 = 125 - 200 ps), free positrons (τ_2 = 300 - 400 ps) and o-Ps pick-off (τ_3 = 1 - 5 ns). Only the third component (o-Ps) responds to material properties: τ_3 = 1640 ps (c = 0, T_g = 122 °C) and 2145 ps (content of comonomer c = 75 wt-

%, $T_g \approx 0$ °C, Fig. 2, [14]). Typical specimens in PALS experiments are platelets of 8x8 mm^2 in area and 1.5 mm in thickness. For each experiment, two identical samples are sandwiched around a 5 MBq positron source (^{22}Na), prepared by evaporating carrier-free ^{22}NaCl solution on a Kapton foil of 8 μm thickness. One experiment lasts between 1 and 10 hours depending on the total count.

Following convolution of $s(t)$ with the resolution function and subtraction of background and source components the spectra can be analysed by a non-linear least squares fit of eq. (6) to the data points N_i. A continuous lifetime distribution may be analysed using the Laplace-inversion routine CONTIN-PALS2 or the maximum entropy routine MELT (see [11] and refs. given therein). The new routine LT9.0 assumes a log-normal distribution of annihilation rates $\alpha(\lambda)$, $\lambda = 1/\tau$, for some, if not all, annihilation channels and calculates the mass centre and width of this distribution.

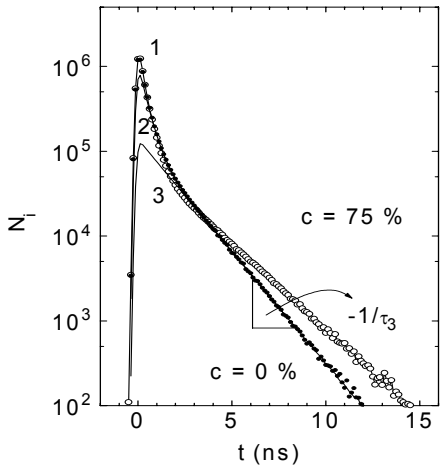

Figure 2. Positron lifetime spectra in CR39-copolymers with 0 and 75 % of comonomer [14].

In amorphous polymers Ps is trapped and confined by holes of the free volume (Anderson localisation, see Fig. 3). The hole size can be estimated using a simple quantum mechanical model which assumes the Ps to be confined in a spherical potential well of radius $r = r_h + \delta r$ and an infinite depth where r_h is the radius of the hole. The Ps has a spatial overlap with molecules within a layer δr of the potential wall. This provides a simple but very useful relationship between the o-Ps pick-off annihilation rate and the hole radius r_h:

$$\lambda_{po} = 1/\tau_{po} = 2ns^{-1}\left[1 - \frac{r_h}{r_h + \delta r} + \frac{1}{2\pi}\sin\left(\frac{2\pi r_h}{r_h + \delta r}\right)\right] \qquad (7)$$

where 2 ns^{-1} is the spin averaged Ps annihilation rate in dense electron systems and δr is empirically derived to be 0.166 nm [7,8]. Similar formulae were derived for cylindrical or cubical holes [12]. Frequently, the hole size is expressed as mean free path of Ps inside the hole. Typically o-Ps lifetimes and holes sizes are $\tau_{po} = \tau_3 = 1$ - 5 ns and $r_h = 2$ - 4 Å ($v_h = 4\pi r_h^3/3 = 50$ - 200 Å^3). In polymer crystals Ps is sometimes formed in interstitial free volumes. In this case, the o-Ps pick-off lifetime reflects the packing coefficient C of the crystals ($C \approx 0.70$, $\tau_3 \approx 1$ ns). The Ps yield in crystals is usually lower than in the amorphous phase or can also completely disappear. Based on eq. (7) the mean size of the free-volume holes may be estimated as a function of temperature, pressure, the content of plasticizer, humidity, or the composition of copolymers and blends etc. The lower detection limit of the method is estimated to be $r_h \approx 1.5$ Å ($v_h \approx 20$ Å^3), while in mesoscopic systems τ_3 values of 100 ns corresponding to $r_h \approx 10$ nm [12] have been observed.

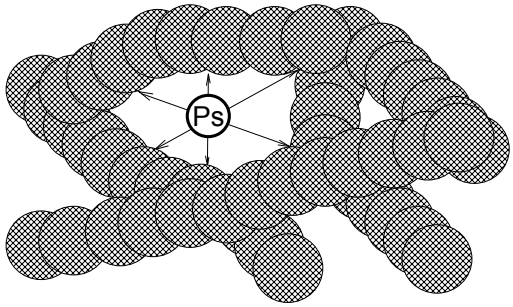

Figure 3. Ps localisation and annihilation in a hole of the (excess) free volume.

3. Application to Polymers

3.1 The Specific Total, Occupied and Free Volume

PALS is able to deliver the mean size and size distribution of free volume holes, but not the number density and volume fraction [13-18]. Frequently the o-Ps intensity I_3 is assumed to be linearly related to the hole density. I_3, however, shows the Ps yield P, $I_3 = 3P/4$, which is affected by various processes such as e^+/e^- trapping by shallow traps and the mobilities of these particles [7,8]. The number density and volume fraction of holes can be obtained, however, from a comparison of PALS with the macroscopic volume obtained from pressure-volume-temperature (PVT) experiments, in particular when these are analysed with the Simha-Somcynsky equation of state (S-S eos) [14-17]. This theory assumes a (hexagonal) lattice with an occupation y of less than 1. The hole fraction, $h = 1 - y = h(T/T^*, V/V^*, P/P^*)$, ($T^*$, V^* and P^* are scaling parameters) is calculated from an equation obtained from the pressure relation $P = -(\partial F/\partial V)_T$, where $F = F(V, T, h)$ is the (Helmholtz) configurational free energy. h can be identified with the fractional (excess) free volume defined previously, $f = V_f/V \equiv h$ [19,20].

We have determined the specific volume from PVT experiments using a fully automated GNOMIX high-pressure (mercury) dilatometer [15]. Fig. 4 shows the specific volume, V, and the specific occupied volume, $V_{occ} = (1 - h)V$, for polystyrene (PS) together

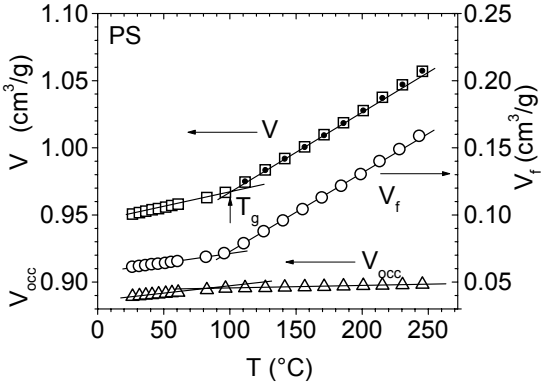

Figure 4. The specific total, V, free V_f, and occupied, V_{occ}, volume of polystyrene (PS) as a function of the temperature T at zero pressure. Open symbols: experimental data, dots: S-S eos fits. (to be published).

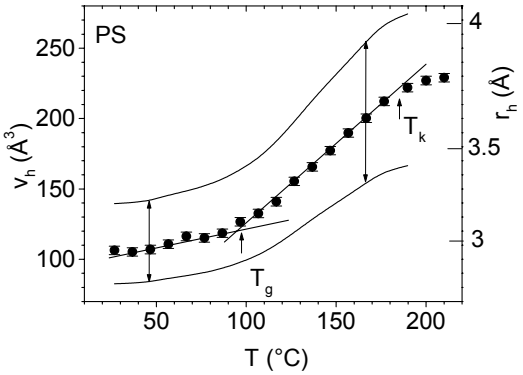

Figure 5. The mean hole volume $v_h(\tau_3)$ and its dispersion ($\pm\sigma$) of PS as a function of temperature T. Above T_k the o-Ps lifetime τ_3 and thus v_h does not anymore represent correctly the true hole volume (see text).

with the specific free volume, $V_f = hV = V - V_{occ}$ as example. V_{occ} includes the interstitial free volume, V_{if}, $V_{occ} = V_W + V_{fi}$, and has at T_g a value of $V_{occ} = 1.45V_W$ that corresponds well to volume typically for crystalline polymers. The coefficient of thermal expansion of the occupied volume, changes at T_g from $\alpha_{occ,g} = 1.0\times10^{-4}$ K^{-1} ($T < T_g$) to $\alpha_{occ,r} = 0.2\times10^{-4}$ K^{-1} ($T > T_g$). This change seems to be unexpected, but is confirmed by the PALS data (Fig. 6).

As can be observed in Fig. 4, the specific volume shows an increase in its coefficient of thermal expansion at T_g from $\alpha_g = 2.25\times10^{-4}$ K^{-1} to $\alpha_r = 6.36\times10^{-4}$ K^{-1}. The corresponding

increase for the free volume is from $\alpha_{fg} = 1.8\times10^{-3}$ K^{-1} to $\alpha_{fr} = 8.4\times10^{-3}$ K^{-1}. The fractional free volume at T_g amounts to $f \equiv h = 0.070$.

Fig. 5 shows the mean hole volume, v_h, calculated from the PALS results via eq. (7). Together with $v_h(\tau_3)$, the boundaries $v_h(\tau_3 - \sigma_3)$ and $v_h(\tau_3 + \sigma_3)$ are shown where σ_3 is the dispersion (standard deviation) of the lifetime distribution obtained from the LT9.0 analysis. Similarly to V_f, the mean volume v_h shows a strong increase in its expansivity at T_g. At low temperatures, o-Ps is trapped in local free volumes within the glassy matrix and τ_3, and hence v_h, show the mean size of static holes. The averaging occurs over the hole sizes and shapes. The slight increase of v_h with temperature mirrors the thermal expansion of free volume in the glass due to the anharmonicity of molecular vibrations and local motions in the vicinity the holes. In the rubbery phase the molecular and segmental motions increase rapidly resulting in a steep rise in the hole size with temperature. Now v_h represents an average value of the local free volumes whose size and shape fluctuate in space and time. The o-Ps lifetime mirrors the mean geometrical hole size as long as the structural relaxation times do not reach the order of magnitude of this lifetime.

The coefficients of thermal expansion of hole volume were estimated to be $\alpha_{hg} = (1.95 \pm 0.2)\times10^{-3}$ K^{-1} ($T < T_g$) and $\alpha_{hr} = (9.5 \pm 0.08)\times10^{-3}$ K^{-1} ($T > T_g$), the hole volume at T_g is $v_{hg} = (121 \pm 2)$ Å^3. The α_{hr} value is larger by a factor of ~15 than of the macroscopic coefficient of thermal expansion, α_r. From this a free volume fraction of $f \approx \alpha_{hr}/\alpha_r = 1/15 = 0.07$ follows. A more accurate estimate of f and of the mean number of holes per mass unit, N_h', may be obtained from one of the relations ([14], see also [15-18]),

$$V_f = N_h' \, v_h \tag{8}$$

$$V = V_{occ} + N_h' \, v_h. \tag{9}$$

Fig. 6 shows the specific total volume, V, and specific free volume, $V_f = hV$, which were plotted vs. the hole volume v_h. One observes that both V and V_f follow linear functions for the data from above T_g with slopes of $N_h' = 0.55$ and $0.53\pm0.02\times10^{21}$ g^{-1}. The values correspond to a hole volume density of $N_h = 0.55$ nm^{-3}. We note that in case of the specific volume curves the values below T_g are increasingly lower with decreasing temperatures than predicted by the extrapolation of the lines from above T_g. This deviation is due to the abrupt increase in the coefficient of thermal expansion of the occupied volume observed in Fig. 4. Both estimates for N_h', from eqs. (8) and (9), agree almost completely.

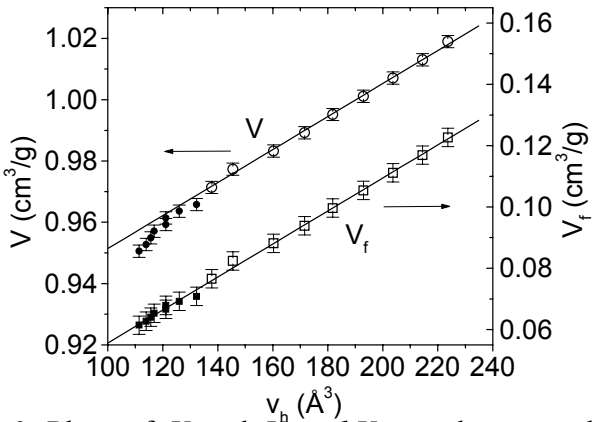

Figure 6. Plots of V and $V_f = hV$, vs. the mean hole volume v_h for PS. The lines are linear fits to the data above T_g and below T_k (open symbols). The filled symbols are data from below T_g.

The constancy of the hole density, N_h', is a surprising and interesting result confirmed by all other works in the literature related to this question [14-18]. It means that the whole

segmental motion above T_g which is allowed by the holes but creates also new holes is mirrored in the mean size (and size distribution) of the local free volumes but not in their mean number density. Due to this, the polymer dynamics as seen, for example, via the polymer viscosity, is observed to be clearly related to the hole size detected by PALS. The same was found to be true for the diffusion of small guest molecules (gases and ions [21,22]) in polymers.

At this point we remark that the S-S eos uses a picture which differs from the structure of the free volume observed by PALS. o-Ps detects individual holes which have a size distributions around a mean value being typically v_h = 100 - 200 Å^3 and a constant hole density N_h'. The S-S model, on the other hand, assumes uniform cells [19,20] of a size estimated for PS to be ω = 60 Å^3. The increase in free volume comes mainly from the creation of new empty cells, their number density, N_h^{SS}, can be described by an Arrhenius law. In estimation of N_h' we assumed $V_f = N_h^{SS}\omega = N_h'v_h$. The agreement of this value with the hole number estimated from the empirical relation $V = V_{occ} + N_h'v_h$ shows that the hole fraction and the specific free volume are correctly estimated by the S-S eos.

Some authors have attempted to overcome this discrepancy in the modelling by assuming that the hole probed by o-Ps represents a cluster of the unoccupied cells described by the S-S eos [5]. The mean hole volume at room temperature corresponds to $v_h/\omega \approx 1.7$ cells, this number increases at 200 °C to 3.3. Due to free volume fluctuation, the number varies at 200 °C between 1 and 5 ($\pm 3\sigma$). Further research may resolve this question.

3.2. Hole Size Distribution and Thermal Volume Fluctuation.

With eq. (7) and the distribution of the annihilation rates, $\alpha(\lambda)$, obtained from the analysis of lifetime spectra using the routine LT, for example, the hole radius probability distribution, $n(r_h) = -\alpha(\lambda)d\lambda_3/dr_h$ ($\lambda_3 = \lambda_{po}$), can be calculated via [8]

$$n(r_h) = -3.32\{\cos[2\pi r_h/(r_h + \delta r)] - 1\}\ \alpha(\lambda)/(r_h + \delta r)^2 \qquad (10)$$

From eq. (10) the fractional hole volume distribution, $g(v_h) = n(r_h)/4\pi r_h^2$, and the number density hole volume distribution, $g_n(v_h) = g(v_h)/v_h$, can be calculated. The $n(r_h)$ and $g_n(v_h)$ distributions are shown in Fig. 7 for PS (to be published). The $n(r_h)$-distributions can be approximated by a Gaussian, while $g_n(v_h)$ shows a shape like a Γ-function. The distributions are normalised to the fractional hole free volume f = 1 where $\int g(v_h)dv_h = \int v_h g_n(v_h)dv_h = \langle v_h\rangle\langle N_h\rangle = f$ (integration from 0 to ∞). Free volume distributions are frequently assumed to follow a Gaussian or a binomial distribution [20] in agreement with our results. The $g_n(v_h)$ of Fig. 7 seems, however, to contradict the exponential distribution function of the Cohen and Turnbull model, eq. (2). We remark however, that the right wing tail of the $g_n(v_h)$ distribution may be fitted by an exponential function. When $n(r_h)$ is described by Gaussian with a larger width, $g_n(v_h)$ will show an exponential-like shape. The discrepancy is usually explained by the lower detection threshold of PALS, estimated to be ~20 Å^3. In ref. [6] the o-Ps lifetime distribution is calculated employing simulations of the amorphous polymer structure.

For comparison with theory we have calculated from the PALS data the root-mean-square fluctuation in the fractional free volume which we define by

$$\delta f_{rms} = (\langle \delta V_f^2\rangle/\langle V\rangle^2)^{1/2}, \qquad \text{where } \langle \delta V_f^2\rangle = \langle N_h'\rangle^2 \langle \delta v_h^2\rangle. \qquad (11)$$

The left hand side of eq. (11) assumes that the fluctuation in N_h' can be neglected compared with the fluctuation in the hole volume v_h. We have calculated $<\delta v_h^2>$ as the variance of the $g_n(v_h)$ distribution. Figure 8 shows that $\delta f_{rms} = (<N_h'>/<V>)<\delta v_h^2>^{1/2}$ varies with the temperature very similarly to $<v_h>$ and $<V_f>$. In thermal equilibrium, above T_g, the spatial fluctuation of the free volume is identical with the time fluctuation. PALS detects these fluctuations as a "static" hole size distribution as long as the relaxation times for segmental motion are smaller than the o-Ps lifetime. Below T_g most of the fluctuations are "frozen-in" and quasi-static.

Following conventional thermodynamics the mean square fluctuation of the volume V about its mean value $<V>$ at equilibrium is related to the second derivative of the Helmholtz free energy F via $<\delta V^2> = -k_B T/(d^2F/dV^2)_{<V>}$ [20]. With $(d^2F/dV^2)_{<V>} = -(dP/dV)_{<V>}$ one obtains the well know relation $<\delta V^2> = k_B T\, \kappa <V>$ and, assuming that the fluctuation in the free and occupied volume are independent,

$$<\delta V_f^2> = k_B T\, \kappa_f <V_f> = k_B T\, \kappa_f^* <V> \qquad (12)$$

where $\kappa_f = -(1/V_f)[dV_f/dP]_T$ is the isothermal compressibility of the free volume and $\kappa_f^* = -(1/V)[dV_f/dP]_T$ the corresponding fractional compressibility. Frequently κ_f^* is approximated by $\kappa_f^* = \Delta\kappa = \kappa_r - \kappa_g$. We have calculated κ_f^* from the pressure dependence of the free

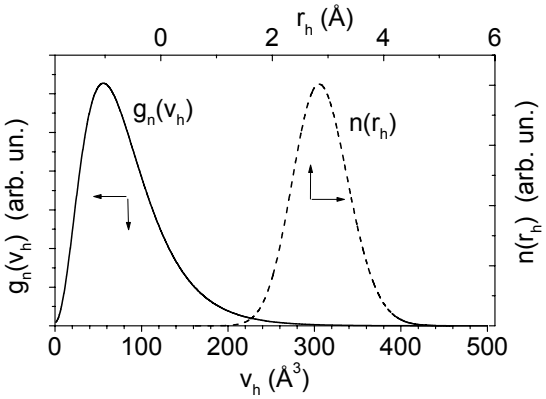

Figure 7. Free volume hole radius distribution, $n(r_h)$, and number density hole volume distribution, $g_n(v_h)$, in PS for $T = T_g = 97$ °C.

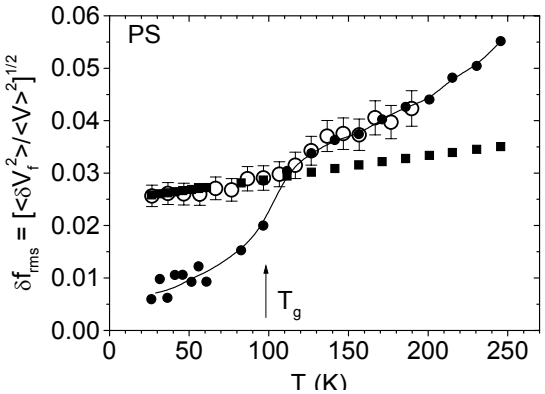

Figure. 8. δf_{rms} derived from the thermodynamic fluctuation (filled circles) and the Robertson theory (filled squares) in comparison with PALS (open circles).

volume, $V_f(T,P)$. An equation similar to eq. (12) has been used to discuss density fluctuations observed by X-ray small angle scattering.

Thermal fluctuations are considered in a subvolume $<V>$ embedded in, and being in thermodynamic contact with, a much larger one [20]. Fig. 8 shows the fit of eq. (12) to the PALS experiments above T_g, which delivers $<V> = 2.15$ (± 0.1) nm^3. This value corresponds to 13 monomer units and is reasonably close to the value of $1/N_h = 1.8$ nm^3, the volume which contains one hole. Below T_g eq. (12) delivers data clearly below the PALS experiments since although eq. (12) can be used as an approximation of the volume fluctuation below T_g, it describes only the dynamic contribution of the disorder while the PALS data are dominated by the static hole size distribution. Fig. 8 shows also calculations using a theory of Robertson [20] which is based on the S-S eos, assuming $<V> = 1.05$ nm^3. Obviously this theory describes well the static free volume distribution but not free volume fluctuations above T_g.

3.3 The Free Volume and the Dynamic Heterogeneity in Glass-forming Liquids

As shown in Fig. 5, at a higher, critical "knee" temperature T_k = 180 °C, the increase of the hole volume with the temperature levels off. This effect is not observed in the macroscopic volume and may be considered therefore as being due to the Ps probe itself. The o-Ps lifetime and the hole size calculated from this no longer mirror the true mean hole size. We observed also a distinct decrease in the width of the hole size distribution above T_k [23]. Possible reasons for this behaviour could be: (i) The existence of Ps in self-trapped "cage" states in the soft matrix of the polymer (Ps bubble). (ii) Thermally exited detrapping of Ps from free volume holes. (iii) The structural relaxation time reaches the order of the o-Ps lifetime of ~ 2 ns leading to a smearing of holes during the life of o-Ps.

Another interpretation is the disappearance of the dynamic and structural heterogeneity of the glass-forming system and transition to a homogeneous liquid. The latter interpretation is of special interest since it relates the free volume properties to a change in the polymer dynamics. Ngai et al. [24] showed for low-molecular materials that at a temperature of $\approx 1.2\ T_g$ (for "fragile" glass forming liquids) to $\approx 1.5\ T_g$ (for "stronger" glasses) the mean square atomic displacements $\langle u^2 \rangle$ of motions with relaxation times shorter than 1 ns increase dramatically. At the same temperatures the PALS "knee" appeared in these materials.

Possibly, the local free volume detected by PALS in polymers may be identified with the high mobility regions (Glarum-Levey defect) inside a co-operatively rearranging regions (CRR) [10]. The typical hole size ($v_h \approx 0.1$ nm^3) and the volume which contains one hole, $1/N_h$ = 1 to 5 nm^3 [14-18], seem to agree with this interpretation. There are, however, two observations which contradict this interpretation. First, the hole density and therefore the value $1/N_h$ are found to be independent on temperature [13-18], while the fluctuation theory estimates its increase when approaching T_g from T_+ [10]. Second, PALS studies of alkyl methacrylates (to be published) delivered T_k values which are distinctly higher than the T_+ values which show a systematic lowering with increasing length of the alkyl side chain [25]. Thus the interpretation of the PALS "knee" as being caused by structural relaxation times in the order of the o-Ps lifetime seem likely. Further research may solve this question.

3.4 Free Volume and Mobility

The relation between the free volume and the polymer mobility is frequently studied by measuring the diffusion properties of small molecules in polymers. Extensive studies of gas diffusion in comparison with PALS can be found in several papers. Recently, we have studied the ionic conduction in ethylene glycol [21] and later in ethylene oxide based polymer (PEO) electrolytes which exhibit single ion (cation - Li^+ or anion - ClO_4^-), and mixed ion (from the dissociation of $LiClO_4$ salt) conduction by employing PALS and conductivity (σ) measurements in the temperature range between 170 and 370K [22]. The conductivity is visualised as being due to a combination of ion/polymer co-operative motion with the occasional independent ion movements; the time scale for the latter is expected to be much shorter than for polymer relaxation.

We found that the hole volume v_h shows a typical glass-transition behaviour for all of the samples. However, indications for two relaxation processes separated in temperature are found. The lower one is attributed to the motion of “free” polymer segments, and the higher one, appearing only in the electrolytes, to segments solvating cations. A discrepancy between the T_g estimated from PALS and DSC, $T_g^{DSC} = T_g^{PALS}$ - (25 to 27) K in case of polymer

electrolytes, can be resolved assuming that the DSC responds mainly on the free segmental motion but PALS on the segmental motion of co-ordinated polymer chains.

We found evidence for the validity of (i) the linear expansion of local free volume from PALS, eq. (4), (ii) the Vogel-Tammann-Fulcher (VTF) law for the ionic conductivity σ, eq. (5), and (iii) the Cohen-Turnbull equation that relates σ to the local free volume v_h , eq. (3). These were found to be valid in the temperature range above the end (or freezing) temperature of the glass transition, $T_{ge} \approx 1.06\ T_g^{PALS}$. Fig. 9 shows the Cohen-Turnbull plots (log σ vs. $1/v_h$) for the Li^+ conduction. Deviations from eq. (3) are observed below T_{ge} and above T_k where PALS does not detect the true hole size. From VTF fits, eq. (5), to σ we obtained a Vogel temperature of $T_0 \approx T_g^{DSC} = T_g^{PALS}$ - (25 to 27) K and pseudo-activation energies of B = 3.7 - 5.7 kJ/mol. The critical temperatures at which the extrapolated conductivity (T_0, Vogel temperature) and the free volume $v_h(T_0')$ disappear, agree each with the other within the error limits. We also observed such agreement when comparing T_0' with the Vogel temperature T_0 of the segmental (α-) relaxation for PS and atactic polypropylene. We could also confirm the relation $B/R = (\gamma v^*/v_m \alpha_f^*)$ (see eqs. 3 - 5, [21, 22]). From the Cohen-Turnbull plots critical hole volumes γv^*, required for an ion transportation, of 1.20 nm^3 (^{R}PEO-Li), 1.09 nm^3 (^{R}PEO-ClO_4), 1.00 nm^3 (^{R}PEO-$LiClO_4$) [22] and 0.9 nm^3 (ethylene glycol - $LiClO_4$ [21]) were estimated. From this it was concluded that γv^* represents the critical free volume for the segmental motion with which the ion transport is associated. Surprisingly, there are no clear effects that could be attributed to the different type of moving ions. This may be considered as an indication that each type of ionic conductivity is associated with the same segmental mobility independent of the specific interaction with the polar polymer chains. We remark that the critical volumes γv^* are far in the right wing of the hole size distributions. This shows again that only the largest holes of the excess free volume contribute to the mobility of chain segments or diffusion of guest molecules in amorphous polymers. Below T_{ge}^{PALS} the conductivity is larger than predicted by the VTF relation [22] which can be described by an Arrhenius-type activation energy.

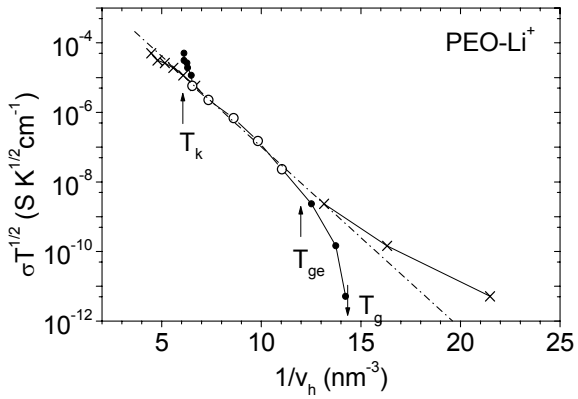

Figure 9. Variation of $\sigma T^{0.5}$ with the reciprocal local free volume, $1/v_h$, estimated from PALS, in ^{R}PEO-Li (Cohen-Turnbull fit). Open and filled circles: v_h as obtained from the experiment, open circles: used from these for the CT fit (dash-dotted line); crosses: v_h as obtained from extrapolation of the linear fit in the range $T_{ge} < T < T_k$. [22]

3.5. Free Volume and Rigid and Mobile Amorphous Phases in Semicrystalline Polymers

Recently we have studied the thermal expansion of free volume holes in semicrystalline ethylene/1-octene copolymers (P(E-co-O)) with a content of 1-octene comonomer between 7 and 24 wt.-% and a crystallinity X_c (from WAXS) between 50 % and 10 % and a high-density polyethylene (HDPE, X_c = 70 %) [26]. The thermal expansion of the hole volume, v_h, in HDPE could be fitted by a parabola and shows no indication of the glass transition (Fig. 10).

From this we concluded that the whole amorphous phase is constrained by the crystals and immobile, $\beta = 1 - X_c = 30$ %. The copolymers show an increasing thermal expansion above T_g which we attribute to an increasing fraction of mobile amorphous phase. By fitting a parabola to the data below T_g and subtracting this from the data above T_g the fraction γ of the mobile amorphous phases can be estimated, $X_c + \beta + \gamma = 1$. Fig. 11 shows how these fractions vary as a function of the content of 1-octene comonomer.

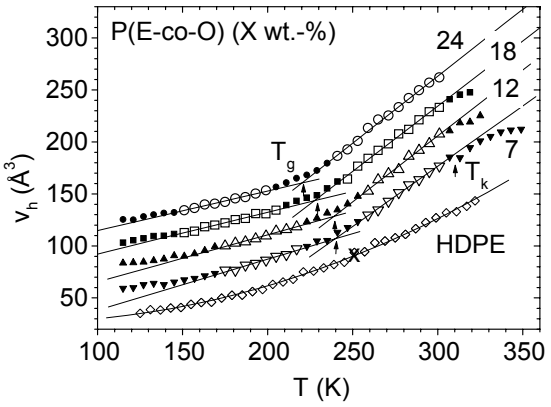

Figure 10. The temperature dependence of the mean local free volume v_h in P(E-co-O(wt.-%)) and HDPE. For clarity the data are shift on the vertical scale by 20 Å^3 each to the other. [26]

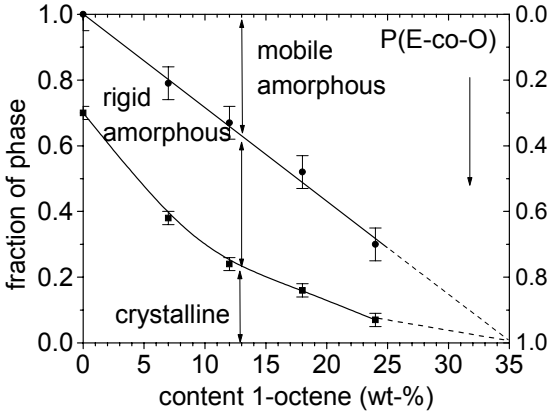

Figure 11. Mass fractions of the crystalline, X_c, the rigid crystalline-amorphous interfacial, β, and the mobile amorphous, γ, phases as a function of the content of 1-octene.

4. Conclusions

Positron annihilation is a unique technique for studying the microstructure of amorphous materials. Employing the lifetime spectroscopy (PALS) the size and size distribution of subnanometer size local free volumes (holes) may be studied. In combination with macroscopic volume data the fractional free volume and the number of holes may be estimated. Several examples for the application to polymers have been given. Close relations between the hole size and the polymer dynamics have been observed.

There are several further applications of the method such as (i) the chemical surroundings of holes sensed by DBAR [27], (ii) the hole anisotropy in highly crystalline fibres detected by ACAR [28], (iii) interdiffusion in demixed polymer blends [29], (iv) humidity sorption into free volume holes in polyimides [30] and polyamide [31], and (v) the study of surface and near-surface properties [32] using slow, monoenergetic positron beams [9]. Employing slow positron beams the change of the glass transition temperature at the surface of polymers and in confined geometries has been observed [8].

References

[1] J. Frenkel, *Kinetic Theory of Liquids*, Oxford University Press, London 1946.
[2] A. K. Dolittle, *J. Appl. Phys*. **1951**, *21*, 1471.
[3] M. L. Williams, R. F. Landel, J. D. Ferry, *J. Am. Chem. Soc*. **1955**, *77*, 3701.
[4] M. H. Cohen, D. Turnbull, *J. Chem. Phys*. **1959**, *31*, 1164; D. Turnbull, M. H. Cohen, *J. Chem. Phys*. **1970**, *52*, 3038.

[5] S. Vleeshouwers, J.-E. Kluin, J. D. McGervey, A. M. Jamieson, and R. Simha, *J. Polym. Sci. B: Polym. Phys.* **1992**, *30*, 1429.
[6] H. Schmitz, F. Müller-Plathe, *J. Chem. Phys.* **2000,** *112,* 1040.
[7] O. E. Mogensen, *Positron Annihilation in Chemistry*, Springer-Verlag, Berlin, Heidelberg, New York, 1995.
[8] Y. C. Jean, P. E. Mallon, D. M. Schrader (Eds.*), Principles and Application of Positron and Positronium Chemistry*, World Scientific, Singapore, 2003.
[9] R. Krause-Rehberg, H. Leipner, *Positron Annihilation in Semiconductors*, Springer Verlag, Heidelberg, 1999.
[10] E.-J. Donth, *The glass transition: Relaxation dynamics in liquids and disordered materials,* Springer-Verlag, Berlin 2001.
[11] G. Dlubek, Ch. Hübner, S. Eichler, *Nucl Instr and Meth B* **1998**, *142*, 191; and *phys stat sol (a)* **1998**, *157*, 351.
[12] D. W. Gidley, W. E. Friece, D. L. Dull, J. Sun, *Appl. Phys. Lett.* **2000**, *76*, 1282.
[13] G. Dlubek, D. Bamford, A. Rodriguez-Gonzalez, S. Bornemann, J. Stejny, B. Schade, M. A. Alam, M. Arnold, *J. Polym. Sci.: Part B: Polym. Phys.* **2002**, *40*, 434.
[14] G. Dlubek, J. Stejny, M. A. Alam, *Macromolecules* **1998**, *31*, 4574.
[15] G. Dlubek, V. Bondarenko, J. Pionteck, M. Supey, A. Wutzler, T. Krause-Rehberg, *Polymer* **2003**, *44*, 1921.
[16] R. Srithawatpong, Z. L. Peng, B. G. Olson, A. M. Jamieson, R. Simha, J. D. McGervey, T. R. Maier, A. F. Halasa, H. Ishida, *J. Polym. Sci.: Part B: Polym. Phys.* **1999**, *37*, 2754.
[17] M. Schmidt, F. H: J. Maurer, *Polymer* **2000**, *41*, 8419;
[18] J. Bohlen, R. Kirchheim, *Macromolecules* **2001**, 34, 4210.
[19] R. Simha, T. Somcynsky, *Macromolecules* **1969**, *2*(4), 342.
[20] R. E. Roberson, *Free-Volume Theory and its Application to Polymer Relaxation in the Glassy State*, In *Computational Modelling of Polymers*, Bicerano, J. Ed.; Marcel Dekker: Midland, MI, 1992, p. 297
[21] D. Bamford, G. Dlubek, A. Reiche, M. A. Alam, W. Meyer, P. Galvosas, F. Rittig, *J. Chem. Phys.* **115**, 7269 (2001).
[22] D. Bamford, A. Reiche, G. Dlubek, F. Alloin, J.-Y. Sanchez, M. A. Alam, *J. Chem. Phys.* **2003,** *118*, 9420.
[23] G. Dlubek, M. Supej, V. Bondarenko, J. Pionteck, G. Pompe , R. Krause-Rehberg, I. Emri, *J. Polym. Sci.: Part B: Polym. Phys.* **2003**, *41*, Nov.
[24] K. L. Ngai, L.-R. Bao, A. F. Yee, C. L. Soles, *Phys. Rev. Lett.* **2001**, *87*, 215901.
[25] M. Beiner, S. Kahle, S. Abends, E. Hempel, S. Höring, M. Meissner, E. Donth, *Macromolecules* **2001**, *34*, 5927.
[26] D. Kilburn, D. Bamford, T. Lüpke, G: Dlubek, T. J. Menke, M. A. Alam, *Polymer* **2002**, *43*, 6973.
[27] G. Dlubek, H. M. Fretwell, M. A. Alam, *Macromolecules* **2000**, *33*,187.
[28] D. Bamford, M. Jones, J. Latham, R. J Hughes, M. A. Alam, J. Stejny, G. Dlubek, *Macromolecules* **2001**, *34,* 8156.
[29] G. Dlubek, J. Pionteck, V. Bondarenko, G. Pompe, Ch. Taesler, K. Petters, R. Krause-Rehberg, *Macromolecules* **2002**, ***35***, 6313.
[30] G. Dlubek, R. Buchhold, Ch. Hübner, A. Naklada, *Macromolecules* **1999**, *32* 2348.
[31] G. Dlubek, F. Redman, R. Krause-Rehberg, *J. Appl. Polym. Sci.* **2002**, *84*, 244.
[32] G. Dlubek, F. Börner, R. Buchhold, K. Sahre, R. Krause-Rehberg, K.-J. Eichhorn, *J. Polym. Sci.: Part B: Polym. Phys.* **2000**, *38*, 3062.